

PHASE FORMATION BEHAVIOR ON MECHANICALLY ACTIVATED ANNEALING OF Al-RICH PERITECTIC Al-Cr COMPOSITIONS

K.Y. Karuna¹, J. Joardar², A.V.L.N.S.H. Hariharan¹ and K. Ram Mohan Rao^{1,✉}

¹Department of Chemistry, GITAM (Deemed to be University), GITAM Institute of Science,
Vishakhapatnam-530045, India

²International Advanced Research Centre for Powder Metallurgy and New Materials (ARCI),
Hyderabad-500005, India

✉Corresponding Author: rammohanrao.k@gmail.com

ABSTRACT

The formation of phases in the Al rich peritectic compositions of Al - Cr system was investigated under mechanical milling (MM) and subsequent annealing. MM led to the formation of nanocrystalline Al (Cr) solid solution and also caused carbon contamination originating from the organic process control agent (PCA). Al₁₁Cr₄ and AlCr₂ phases were formed on annealing instead of the equilibrium peritectic compounds. Additionally, AlCr₂C phase was also detected after annealing of Al-16 to 33Cr whereas Al-13Cr did not produce any intermetallic compound. The generation of the intermetallic phases was attributed to classical theories of nucleation and growth.

Keywords: Al-Cr System, Peritectic, Mechanical Alloying, Nanocrystalline, Phase Transformation

RASAYAN J. Chem., Vol. 15, No.2, 2022

INTRODUCTION

The Binary Al-Cr phase diagram presents an interesting system as it has a series of peritectic phases.^{1,2} Al-Cr intermetallic coatings are known to provide excellent hardness³, wear and corrosion resistance.^{4,5} Thus, their formation has been studied extensively in the past.⁶⁻¹²

Most of the previous studies have investigated the formation of the Al-Cr intermetallic phases under equilibrium conditions from Al-Cr melts. Few studies have dealt with their formation by mechanical alloying (MA) or mechanically activated annealing (MAA).^{13,14} Archana *et al.* showed the formation of Al₈Cr₅ and Al₁₆Cr₁₀ on MAA of Al-40at.%Cr blend.¹³ Ternary AlCr₂C MAX phase was also observed in this study where carbon originated from the liquid process control agent, toluene. Similarly, Kaurna *et al.* established the formation of various Al-Cr intermetallics and AlCr₂C phases by MAA of Al-33Cr blend.¹⁴ Formation of the peritectic phase is often absent due to slow diffusion during non-equilibrium rapid solidification of liquid melt or solid-state processing by MA or MM. Table-1 shows a few binary peritectic phases observed on the annealing of the ball-milled blend.

Table-1: Few Peritectic Phases on MA or Post-MM Heat Treatment of Binary Systems.

System	x (at.%)	Expected Phase	Phase(s) after MM/MA	Milling Media	Phase(s) after Annealing	Ref.
Al-xTi	50 52	AlTi AlTi	Al(Ti) γ-AlTi + α ₂ -Al ₃ Ti	WC SS	γ-AlTi + α ₂ -Al ₃ Ti -	Al- Dabbagh <i>et al.</i> ¹⁵ Bernatikova <i>et al.</i> ¹⁶
Al-xNi	37 25	Al ₃ Ni ₂ Al ₃ Ni	AlNi Al ₃ Ni	NA SS	Al ₃ Ni ₂ -	Krasnowski <i>et al.</i> ¹⁷ Ying <i>et al.</i> ¹⁸
Al-xCr	40 33	Al ₈ Cr ₅ Al ₉ Cr ₄	Al(Cr) Al(Cr)	WC WC	Cr _{9.5} Al ₁₆ Cr ₁₀ Al ₁₆	Archana <i>et al.</i> ¹³ Karuna <i>et al.</i> ¹⁴

WC: Tungsten carbide, SS: Stainless steel

The formation of these phases could be triggered by improved interdiffusivity during annealing. The phase formation during MA may also be influenced by the presence of iron contamination, which is usual during MA/MM in SS media.¹⁹⁻²¹ The present paper evaluates the phase formation behavior of the Al-enriched Al-Cr system with peritectic compositions under MAA.

EXPERIMENTAL

Powder blends of chromium (CERAC; 99.5% purity; -325 mesh size) and aluminum (Alfa Aesar; 99.5% purity; -325 mesh size) with the composition Al-X at % Cr ($x=13, 16, 19, 33$) were subjected to MM using Pulverisette -P5 (Fritsch GmbH, Germany). The selected compositions are indicated in the phase diagram shown in Fig.-1. The milling of the powder blend was performed in the toluene bath in the vials made of tungsten carbide for 20 hours at 200 rpm. At 10:1 ball-to-powder ratio (BPR) was maintained with 10mm size tungsten carbide balls. The powder obtained after milling was then dried and loaded in a horizontal tubular furnace for annealing under vacuum (10^{-3} Torr) at 600°C for 2 hours. The phase evolution samples were subjected to detailed X-ray diffraction (XRD) using a Smart Lab system (Rigaku Corp., Japan). The powder morphology was studied by scanning electron microscopy (SEM S-3400N, Hitachi, Japan) while thermal analysis was performed with Netzsch STA 449 F3 thermal analyzer.

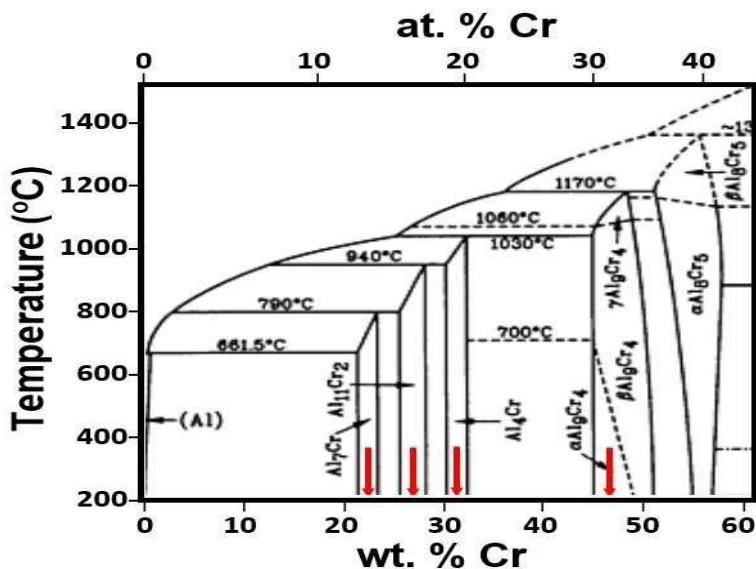


Fig.-1: Al-Cr Phase Diagram indicating the Compositions Studied¹

RESULTS AND DISCUSSION

It is evident from the XRD patterns of Al-Cr blends obtained as a result of MM as shown in Fig.-2 that no Al-Cr intermetallic phase formed after MM as also observed earlier.^{13,14} However, peak broadening and shift were observed indicating grain refinement, defect formation as well as interdiffusion. The crystallite sizes of the phases, as estimated by Warren-Averbach's Fourier method²² are given in Table-2. Interestingly, Table-2 reflects that crystallite sizes of both Al and Cr tend to decrease with an increase in the Cr content. Possibly this indicates higher dissolution of Cr in Al and Al in Cr, leading to hardening of the Al-Cr solid solution and consequently greater size refinement. However, SEM studies (Fig.-3) revealed considerable agglomeration with the increase in the Cr content. It is plausible that the agglomeration took place at a later stage of milling while the crystallite size refinement occurred in the early stages. Monitoring of the crystallite sizes and agglomeration with milling was beyond the scope of the present work.

The MM samples were subjected to thermal analysis up to 850°C at 10°C/min under Argon atmosphere. A distinct difference was observed in Al-13Cr when compared to the rest. As shown in Fig.-4, the Al-13Cr sample showed no significant peak before an endothermic peak at 660°C, which is the melting point of Al. On the other hand, the rest of the samples showed distinct exothermic peaks below 600°C as in the case of Al-33Cr (Fig.-4).

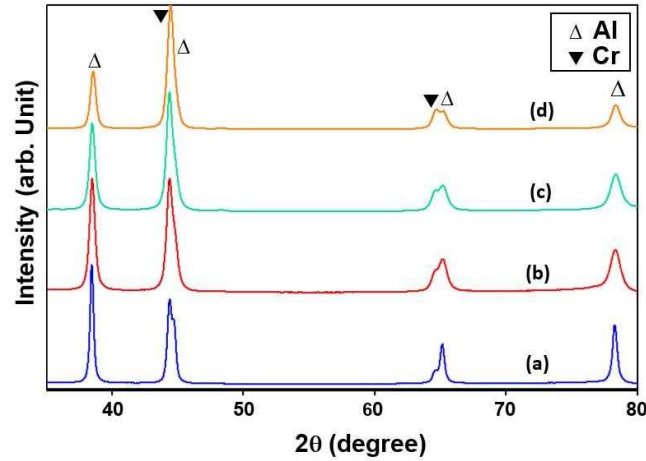


Fig.-2: XRD Patterns of Al-X at.% Cr, MM for 20h for X = (a) 13, (b) 16, (c) 19, (d) 33.

Table-2: Crystallite Sizes (in nm) of the milled Samples by Warren-Averbach's Method

Sample Designation	Crystallite Size of (Al)	Crystallite Size of (Cr)
Al-13Cr	26.1±0.1	21.0±0.2
Al-16Cr	15.8±0.3	18.5±0.2
Al-19Cr	14.6±0.1	18.4±0.3
Al-33Cr	12.2±0.4	16.1±0.1

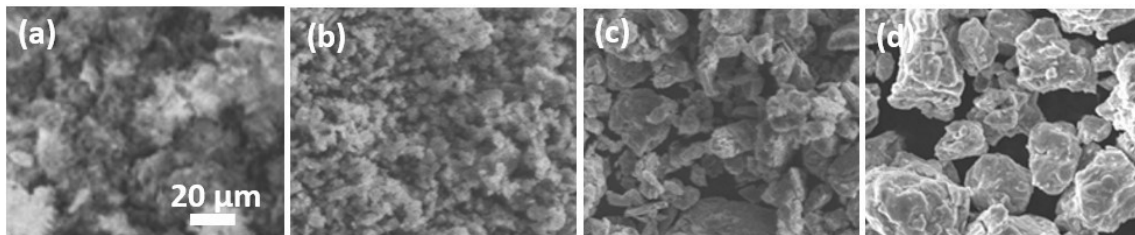


Fig.-3: SEM of Al-X at.% Cr Samples (MM for 20h) with X= (a) 13, (b) 16, (c) 19, (d) 33

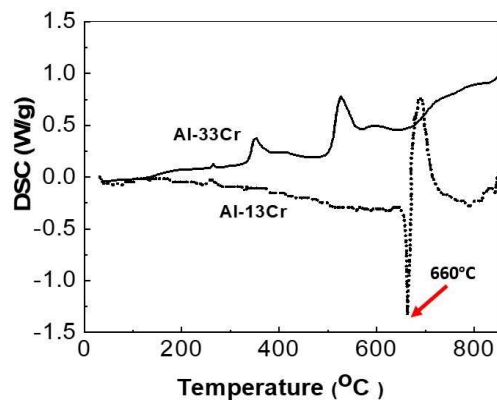


Fig.-4: Typical Thermal Analysis Plots for Al-13Cr and Al-33Cr Ball milled Blends.

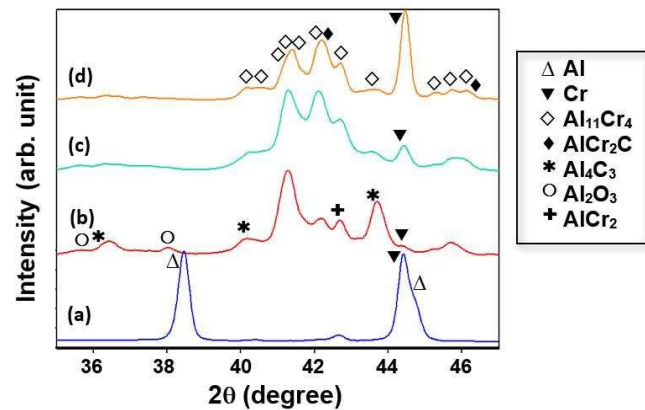


Fig.-5: XRD Patterns of Al-X at.% Cr (MAA-600 °C) with X = (a) 13, (b) 16, (c) 19, (d) 33.

Therefore, all powder samples were compacted at 20MPa load and subjected to heat treatment at 600°C in order to ascertain the phase formation occurring at elevated temperature treatment.

As evident from Fig.-5, Al-13Cr showed no intermetallic compound even after annealing. The only visible change was the shift in the peak positions of Al and Cr when compared to pre-milled and post-milled blends. The remaining Al-XCr blends with X=16, 19 and 33 showed the formation of Al₁₁Cr₄ phase.

The Al-33Cr shows the maximum fraction of Al₁₁Cr₄. The other major phases observed in Al-19 and 33Cr are the AlCr₂C MAX phase and Cr solid solution. It may be noted that the AlCr₂C phase formed due to the presence of about 2.1 and 2.4wt.% of carbon in Al-19Cr and Al-33Cr, respectively, as ascertained by LECO carbon-sulfur analyzer. The previous works^{13, 14} showed that the carbon originates from the degradation of toluene, which is used as PCA. Surprisingly, Al-16Cr showed the insignificant amount of the AlCr₂C MAX phase and Cr-solid solution. Instead, it showed AlCr₂ and Al₄C₃ in addition to a small fraction of Al₂O₃. The presence of low carbon (1.6wt.% in Al-16Cr and 0.5wt.% in Al-13Cr) led to a small fraction of AlCr₂C in Al-16Cr and the absence of the phase in Al-13Cr. Small fraction of AlCr₂C possibly led to the presence of AlCr₂ in Al-16Cr.

The formation of Al₁₁Cr₄ (Space group: *P-1*) in Al-(16-33)Cr is interesting as the existence of this phase is not mentioned in the phase diagram (Fig.-1).¹ However, the phase was identified in Al-rich composition at around Al-25 at. % Cr composition in recent version of the phase diagram, which indicates its formation by a peritectoid reaction between Al₄Cr and α -Al₈Cr₅.^{23, 24} Formation of Al₁₁Cr₄ phase was also reported earlier on annealing of Al-Cr composite film at 690°C.²⁵ The present work shows that Al₁₁Cr₄ exists in an extended phase field between 16 to 33 at.%Cr on MAA.

It may be further noted that the inability to synthesize intermetallic phases in the Al-Cr blends in MM could be possibly influenced by the low diffusivity in Al-Cr system. Figure-6 shows the diffusivity of a few selected elements viz. Cr, Ti, Fe, Ni and V in Al, as estimated from the standard data.^{26, 27} It appears that the diffusivity of elements like Cr, Ti and V in Al would be significantly less at the temperatures encountered by the entrapped powders during MM (blue/dark band)²⁸ when compared to those for elements like Fe and Ni in Al. If we look into the previous efforts on peritectic phase formation during MA (Table-1), it is clear that although the formation of intermetallics in Al-Ni was well reported, the Ti and Cr aluminides were difficult by MA and usually required post-annealing. The inability of MAA at 600°C to induce any phase formation in Al-13Cr could be due to relatively larger crystallite size after ball milling (Table-2). The lower concentration of Cr in Al could also inhibit phase formation as per classical theories of diffusion-induced nucleation. As per these theories, for the phase nucleation, the concentration gradient must drop below a critical level while for its growth; the expected thickness must be higher than a certain critical level.²⁹

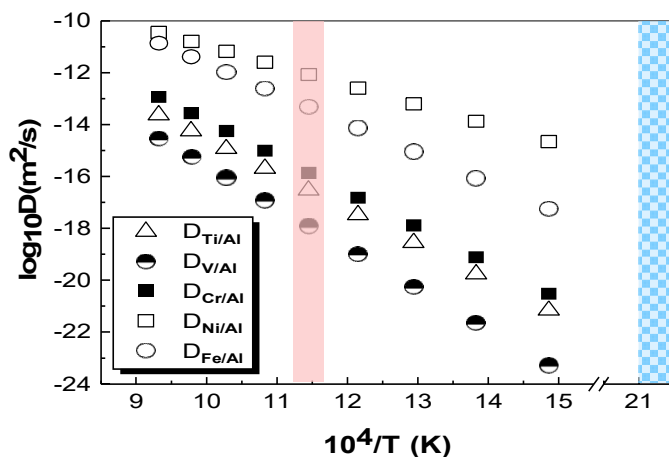


Fig.-6: Diffusivity of Various Elements in Al at Different Temperatures

CONCLUSION

MM was ineffective in the synthesis of Al-rich peritectic phases in Al-X at.%Cr (X=13, 16, 19, 33). MAA at 600°C led to peritectoid Al₁₁Cr₄ phase in the composition range of Al-16 to 33at.%Cr instead of the expected peritectic phases. The formation of AlCr₂C MAX phase was also observed in these compositions. MAA at 600°C was ineffective in any intermetallic formation in Al-13Cr due to the coarser crystallite size of the ball-milled blend. AlCr₂C phase was also absent in Al-13Cr due to low available carbon (0.5 wt. %).

ACKNOWLEDGEMENT

Authors are thankful to GITAM (Deemed to be University) for the encouragement to perform this work and for granting permission to publish.

REFERENCES

1. J. L. Murray, *Journal of Phase Equilibrium*, **19**, 368(1998), <https://doi.org/10.1361/105497198770342120>.
2. G. Kurtuldu, P. Jessner, M. Rappaz, *Journal of Alloys and Compounds*, **621**, 283(2015), <https://doi.org/10.1016/j.jallcom.2014.09.174>
3. Y.L. Su, K.W. Cheng, J. Mayer, T.E. Weirich, A. Schwedt, Y.F. Lin, *Advances in Mechanical Engineering*, **7**, 1 (2015), <https://doi.org/10.1177/1687814015593442>
4. R. Yang, Q. Wu, S. Li, S. Gong, *Procedia Engineering*, **27**, 976(2012), <https://doi.org/10.1016/j.proeng.2011.12.544>
5. Ma Biao, Luo Bin, Wang Zhuozheng, Meng Chuiyi and He Xiujie, *Frontiers in Energy Research*, **9**, 1 (2021), <https://doi.org/10.3389/fenrg.2021.622708>
6. C. Zhang, P. Lv, H. Xia, Z. Yang, S. Konovalov, X. Chen, *et al.*, *Vacuum*, **167**, 263(2019), <http://doi:10.1016/j.Vacuum.2019.06.022>
7. Li Chong, Xu Xiaojing, Wang Saifu, Cai Chengbin, Ju Shihao, Huang Jindong and Yang Song, *Materials Research Express*, **6**, 046426(2019), <https://doi.org/10.1088/2053-1591/aaff03>
8. Song Zeng, Pengcheng Li, Junhua Tian, Chen Chen, Yan Meng, Chaowen Zhu, Huahai Shen, Xiaochun Han, Haibin Zhang, *Corrosion Science*, **198**, 110115(2022), <https://doi.org/10.1016/j.corsci.2022.110115>
9. Jiaojiao Ma, Chuiyi Meng, Hui Wang and Xiujie He, *Coatings*, **11**, 1434 (2021), <https://doi.org/10.3390/coatings11121434>
10. Jiayi He, Xuefeng Liao, Xuexia Lan, Wanqi Qiu, Hongya Yu, Jiasheng Zhang, Wenbing Fan, Xichun Zhong, Zhongwu Liu, *Journal of Alloys and Compounds*, **870**, 159229(2021), <https://doi.org/10.1016/j.jallcom.2021.159229>
11. M. Audier, M. Durand-Charre, E. Laclau, H. Klein, *Journal Alloys and Compounds*, **220**, 225(1995), [https://doi.org/10.1016/0925-8388\(94\)06010-X](https://doi.org/10.1016/0925-8388(94)06010-X)
12. G. Muthusamy, MS Thesis, MIT, USA (2020)
13. M.S. Archana, N. Hebalkar, K. Radha, J. Joardar, *Journal of Alloys and Compounds*, **501**, 18(2010), <https://doi.org/10.1016/j.jallcom.2010.04.046>
14. K.Y. Karuna, J. Joardar, A.V.L.N.S. Hariharan, K. Ram Mohan Rao, *Transaction of Indian Institute of Metals*, **74**, 2313(2021), <https://doi.org/10.1007/s12666-021-02324-4>
15. J.B.Al-Dabbagh, R.M. Tahar, M. Ishak, S.A. Harun, *International Journal of Nanoelectronics and Materials*, **8**, 23(2015)
16. A. Bernatikova, P. Novak, F. Prusa, *Acta Physica Polonica A*, **134**, 733(2018), <https://doi.org/10.12693/APhysPolA.134.733>
17. M. Krasnowski, T. Kulik, *Solid State Phenomena*, **203**, 272(2013), <https://doi.org/10.4028/www.scientific.net/SSP.203-204.272>
18. D.Y. Ying, D.L. Zhang, *Material Science Technology*, **17**, 815(2001), <https://doi.org/10.1179/026708301101510582>
19. Joardar, S.K. Pabi, B.S. Murty, *Journal of Alloys and Compounds*, **429**, 204(2007), <https://doi.org/10.1016/j.jallcom.2006.04.045>

20. S. Perumal, S. Gorsse, U. Ail, M. Prakasam, B. Chevalier, A.M. Umarji, *Journal of Material Science*, **48**, 6018(2013), <https://doi.org/10.1007/s10853-013-7398-2>
21. I. Moravcik, A. Kubicek, L.M. Gouvea, O. Adam, V. Kana, V. Pouchly, A. Zadera, I. Dlouhy, *Metals*, **10**, 1186 (1-15) (2020).
22. B.E. Warren, B.L. Averbach, *Journal of Applied Physics*, **21**, 595(1950), <https://doi.org/10.1063/1.1699713.23>
23. B. Grushko, B. Przepiorzynski, E. Kowalska-Strzeciwillk, M Surowiec, *Journal of Alloys and Compounds*, **420**, L1-L4(2006), <https://doi.org/10.1016/j.jallcom.2005.10.046>
24. H. Okamoto, *Journal of Phase Equilibrium and Diffusion*, **29**, 112 (2008)
25. H. Wu, M. Zhang, B. Xu, G. Ling, *Journal of Alloys Compounds*, **610**, 492(2014), <https://doi.org/10.1016/j.jallcom.2014.05.022>
26. Y. Du, Y. A. Chang, B. Huang, W. Gong, Z. Jin, H. Xu, Z. Yuan, Y. Liu, Y. He, F.Y. Xie, *Material Science and Engineering A*, **363**, 140 (2003), [https://doi.org/10.1016/S0921-5093\(03\)00624-5](https://doi.org/10.1016/S0921-5093(03)00624-5)
27. A. Paul, S. Divinski (Eds), *Handbook of Solid State Diffusion*, Vol. 2: Diffusion Analysis in Material Application, Elsevier, USA (2017)
28. J. Joardar, S. K. Pabi, B. S. Murty, *Scripta Materialia*, **50**, 1199(2004), <https://doi.org/10.1016/j.scriptamat.2004.02.011>
29. G. W. Cox, Ph. D. Thesis, Univ. New South Wales, Australia (1965).

[RJC-6850/2021]